

Low-temperature properties of $\text{La}_{1-x}\text{Ca}_x\text{MnO}_3$ single crystals: Comparison with $\text{La}_{1-x}\text{Sr}_x\text{MnO}_3$

T. Okuda and Y. Tomioka

Joint Research Center for Atom Technology (JRCAT), Tsukuba 305-0046, Japan

A. Asamitsu

Cryogenic Center, University of Tokyo, Tokyo 113-0032, Japan

Y. Tokura

*Joint Research Center for Atom Technology (JRCAT), Tsukuba 305-0046, Japan
and Department of Applied Physics, University of Tokyo, Tokyo 113-8656, Japan*

(Received 13 September 1999)

We have investigated, in single crystals of $\text{La}_{1-x}\text{Ca}_x\text{MnO}_3$, the insulator-metal (IM) transition at the ground state induced by carrier doping or applying pressure around the critical doping level ($x_c \approx 0.22$). The up turn of the resistivity in the IM critical region has been found under a pressure below the Curie temperature (T_C) perhaps due to the proximity to the orbital-ordered ferromagnetic insulating phase. Around the IM transition the additional T^3 and $T^{1.5}$ components are clearly observed in the specific heat, while the T^2 coefficient of the resistivity and the residual resistivity is much enhanced in the metallic region in the vicinity of the transition. These results reveal the subsistence of the charge/orbital correlation in the metallic ground state.

I. INTRODUCTION

The electronic, magnetic, and thermal properties of perovskite-type manganese oxides $R_{1-x}A_x\text{MnO}_3$ (R and A , respectively being a trivalent rare-earth ion and a divalent ion) have been investigated extensively by workers interested in understanding such intriguing phenomena¹ as colossal magnetoresistance (CMR) and charge/orbital ordering. These investigations have revealed an important interplay among the charge, spin, lattice, and orbital degrees of freedom in addition to the well-known spin-charge coupling essential to the double-exchange mechanism.²⁻⁵ It is worth noting that this strong mutual coupling plays a crucial role in the charge and spin dynamics not only around T_C , where it contributes to CMR,⁵ but also in the metallic ground state.⁶⁻⁸ The metallic ground state in the manganite should be recognized as a novel state relevant to the spin-less (that is, fully spin-polarized) electrons where scattering channel via lattice or orbital correlations subsists.⁹

In a relatively wide bandwidth system like $\text{La}_{1-x}\text{Sr}_x\text{MnO}_3$ (LSMO) among these perovskite manganites, the transition from a ferromagnetic (FM) insulator with orbital order to FM metal with orbital disorder occurs around some critical doping level x_c in the ground state.⁶⁻⁸ An anomalous feature is expected to show up near the IM transition because of the critical enhancement of fluctuation of orbital or lattice degrees of freedom.¹⁰ In this paper, we have used high-quality single crystals to investigate, in the most prototypical CMR system, $\text{La}_{1-x}\text{Ca}_x\text{MnO}_3$ (LCMO),¹¹ the IM transition induced by carrier doping procedure or by applying hydrostatic pressure. In particular, we investigated the nature of the ground state by measuring the low-temperature transport and the specific heat. We have compared the results with those observed for the maximal-bandwidth system $\text{La}_{1-x}\text{Sr}_x\text{MnO}_3$ (LSMO) (Refs. 6 and 8) and have clarified

the universal features in the IM critical region and in the metallic ground state of manganites.

The format of this paper is as follows. In Sec. II, we describe the experimental procedures, including the crystal growth procedure, the high-pressure experiments, and specific heat measurements. The results of the resistivity measurements are described in Sec. III, where we overview the transport properties around the insulator-metal (IM) transition in LCMO and LSMO. In Sec. IV, we describe the results of specific heat measurements under a magnetic field and discuss the x dependence of the electronic, lattice, and magnetic contributions at low temperatures near the IM transition. Section V is devoted to a comprehensive discussion of critical behaviors of the IM transition both for LCMO and LSMO. Conclusions are given in Sec. VI.

II. EXPERIMENT

Single crystals of LCMO ($0.1 < x < 0.35$) (Ref. 12) were grown, by the floating-zone method and at a feeding speed of 2 - 5 mm/h, from stoichiometric mixtures of La_2O_3 , CaCO_3 , and Mn_3O_4 that were first ground and then calcined at 1050 °C for 24 h. After this grinding and calcining procedure was repeated several times the resulting powder was pressed into a rod 60-mm long and 5 mm in diameter under a pressure of 2 t/cm² and then sintered at 1350 °C for 24 h. When the x was less than 0.25 the rod could be melted congruently in a flow of air; when x was greater than 0.25 it was melted in a flow of O_2 . Powder x-ray diffraction measurements and electron-probe microanalysis indicated that the single-phase crystals were obtained and that the $\text{Ca}/(\text{La}+\text{Ca})$ ratio was about 0.01 smaller than the corresponding mixture from which the crystal was grown.¹² The oxygen content by redox titration was almost equal to the stoichiometric value.

Resistivity was measured using the conventional four-probe method. The typical cuboidal sample measured 2×4

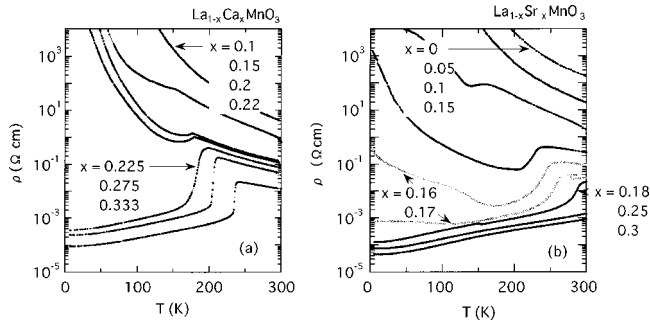


FIG. 1. Temperature dependence of the resistivity of (a) $\text{La}_{1-x}\text{Ca}_x\text{MnO}_3$ (LCMO) and (b) $\text{La}_{1-x}\text{Sr}_x\text{MnO}_3$ (LSMO) with various x values around IM transition.

$\times 0.5$ mm, and electrode was used to make the heat-treatment-type silver paint on it. A quasi-hydrostatic pressure was produced by a clamp-type piston cylinder cell using Fluorinert as the pressure-transmitting medium. The pressure values given in this paper are those measured at room temperature. Pressure calibration indicates that the actual pressure at temperatures below 30 K is 80% of the nominal room-temperature value.¹³ The sample temperature was monitored with a AuFe(0.07%)-Chromel thermocouple placed in the sample room and was increased or decreased at 10 K/h in a whole temperature region.

The specific heat of the same crystals used in the transport measurements was measured in a ^3He cryostat at temperatures from 0.5 to 10 K and under magnetic fields up to 9 T, by using the relaxation method. The specific heat measurements were calibrated by measuring the heat capacity of 99.999% pure copper with and without a magnetic field.

III. TRANSPORT PROPERTIES

The temperature dependence of resistivity for single crystals of LCMO and LSMO with various doping levels x is shown in Fig. 1. Previous studies^{8,13} showed that when x is increased the IM transition in LSMO occurs at an x value approximately equal to 0.16, accompanying the weak localization effect. In the IM critical region where x is between 0.16 and 0.18, the resistivity upturn appears in the metallic state below T_C as seen in Fig. 1(b). When x and pressure are increased, this upturn gradually disappears.¹³ Corresponding to the gradual disappearance of the up-turn, the Fermi surface emerges as manifested by the gradual increase of the electronic specific heat coefficient γ (Ref. 8) [see also Fig. 5(b)]. Thus, the resistivity upturn is ascribed to the proximity to the FM insulating phase where some charge and/or orbital ordering occurs.^{14–18} The remnant of such ordering appears to shrink the Fermi surface in the IM critical region. In LCMO, on the other hand, a sharp IM transition is evident at x between 0.22 and 0.225 and the intermediate state with resistivity upturn could not be observed with the present x -interval ($\Delta x = 0.005$).

To search for the thermally induced IM phenomena near x_c , we performed the hydrostatic pressure experiments, since pressure plays a role similar to that of the carrier doping procedure in the light of increase of the carrier kinetic energy^{13,19,20} and can realize the fine-tuning in the IM critical region as demonstrated previously for LSMO.¹³ The tem-

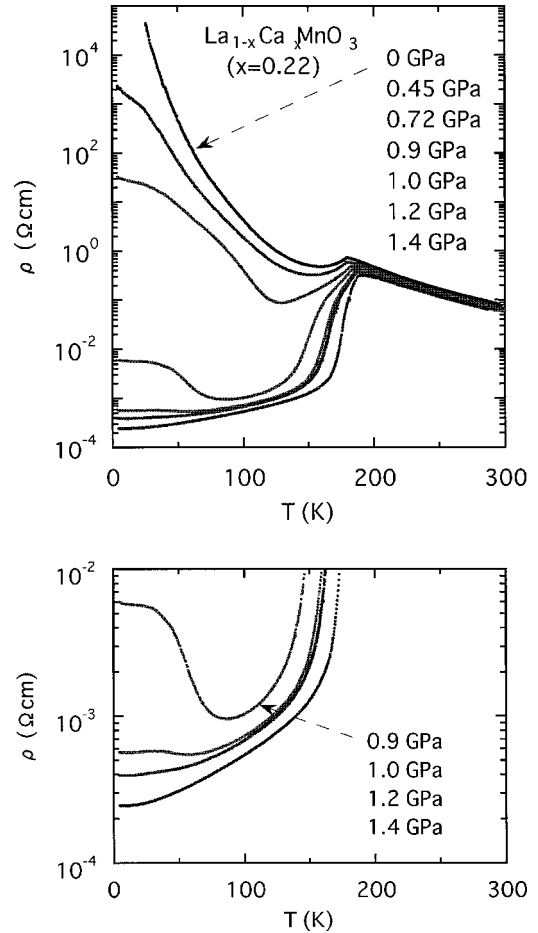


FIG. 2. Temperature dependence of the resistivity for a $x = 0.22$ of LCMO single crystal at various quasi-hydrostatic pressures. The lower panel is a magnification of a low-resistivity region in the upper panel.

perature dependence of resistivity measured under several pressures is shown for LCMO with $x = 0.22$, which is insulating though close to the IM transition, in Fig. 2. When the pressure increases, the resistivity decreases suddenly and T_C increases gradually, while the resistivity upturn is left below T_C even after the IM transition. The resistivity upturn in the IM critical region is gradually suppressed with the increase of pressure and finally disappears above 1.4 GPa. From the continuous disappearance of the upturn and the analogy to the case of LSMO, we might think that the upturn comes from the remnant charge and/or orbital ordering in the FM insulating phase.

In the FM metallic region of LCMO ($x > 0.225$), where residual resistivity is considerably high ($1 - 3 \times 10^{-4} \Omega\text{cm}$), the short-range ordering or correlation of the charge and orbital ordering is likely to persist and make the metallic state anomalous. The temperature dependence of the resistivity in the metallic region is shown in Fig. 3 for crystals with various x values and for various hydrostatic pressures. The FM metallic state appears when x is above 0.225, where the resistivity is almost proportional to T^2 at low temperatures.^{21,22} The dashed line in Fig. 3 represents the results obtained under 1.4 GPa with the compound for $x = 0.22$, for which the resistivity is also proportional to T^2 , indicating the occurrence of the complete IM transition induced by the hydro-

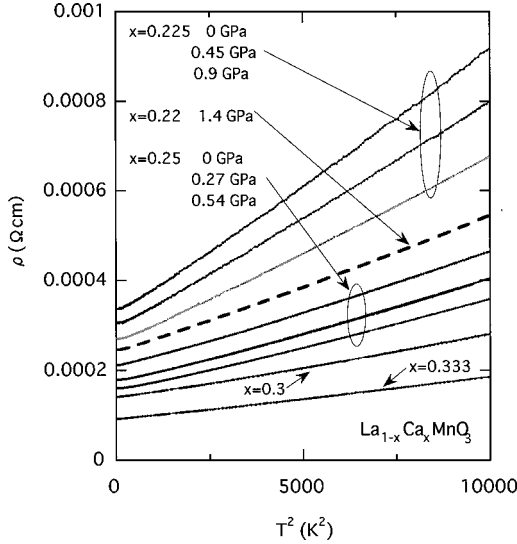


FIG. 3. Temperature dependence of the resistivity at low temperatures in the FM metallic region in LCMO. The resistivity shows roughly T^2 dependence and the residual resistivity ρ_0 decreases significantly with increasing x and pressure.

static pressure. As shown in Fig. 4(a) the T^2 coefficient A is much enhanced near the IM transition and decreases with increasing x or pressure, while as shown in Fig. 4(b) the residual resistivity ρ_0 gradually decreases with increasing x or pressure. Note that although these tendencies are also observed in LSMO,^{6,13} they are much more pronounced in LCMO. The coefficient A is plotted against the residual resistivity ρ_0 in Fig. 4(c), where in both LCMO and LSMO it seems to be related to the residual resistivity by a universal scaling law such as $A \propto \rho_0^{1.6}$ [solid line in Fig. 4(c)]. In the conventional Fermi liquid picture ρ_0 is *not* renormalized by electron correlation or by electron-phonon interaction, in contrast to the case of the electronic specific heat (γ) or the coefficient A , as long as the concentration of ‘impurity’ as a carrier scatter is kept constant.²³ Therefore, the strong correlation between ρ_0 and A as observed even under pressures indicates unconventional nature of the metallic ground state as will be argued in the following sections.

IV. SPECIFIC HEAT

In this paper, we confine our considerations to the data gathered at temperatures above 2 K, where the contribution of the Schottky component of the Mn nucleus is negligible. In the absence of the magnetic field and spin-wave gap, the specific heat in the FM metallic state in the low-temperature region is expressed as

$$C = \gamma T + \beta T^3 + \alpha T^{1.5}, \quad (1)$$

where γ is the electronic specific heat coefficient and the constant β relates to the Debye temperature Θ_D ($\propto \beta^{-1/3}$). The third term expresses the contribution of spin wave in the ferromagnetic state. The coefficient α is proportional to $D^{-1.5}$, where D is the spin-stiffness constant. Here, we explain how these three terms can be decoupled, and we discuss each term separately.

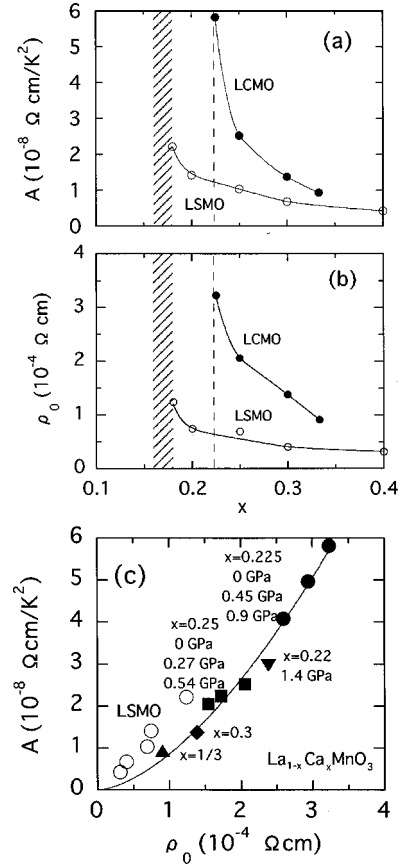


FIG. 4. The x -dependence of (a) the T^2 coefficient A of the resistivity and (b) the residual resistivity ρ_0 in $\text{La}_{1-x}\text{Ca}_x\text{MnO}_3$ (LCMO). A vs ρ_0 is plotted in (c). Solid lines in (a) and (b) are merely guides to the eyes. The curve in (c) was drawn assuming that $A \propto \rho_0^{1.6}$. Solid lines are merely the guide to the eyes. A hatched vertical bar indicates the insulator-metal (IM) transitional region of LSMO, where the resistivity up turn is observed at a temperature lower than T_C . A dashed line indicates the IM phase boundary of LCMO.

The results of measuring the specific heat of LCMO under 0 and 9 T in LCMO are plotted in Fig. 5(a) as C/T versus T^2 for various x values. The decrease of specific heat measured under a 9 T magnetic field is due to the suppression of the thermal excitation of the spin wave in the presence of the field-induced gap, which is also observed for LSMO.⁸ The x variation of the field-induced change directly reflects the x variation of the spin-stiffness constant D (Ref. 24). In a field of 9 T, an energy gap of about 12 K is opened in the spin-wave dispersion so that the spin-wave excitation least contributes to the specific heat at very low temperatures below 4 K. Then, the extrapolated C/T -value at 0 K in 9 T expresses the coefficient of the intrinsic T -linear term, i.e., the electronic specific heat coefficient γ (Ref. 8).

Figure 5(b) shows the x dependence of the γ values for LCMO and LSMO. The γ value for LCMO is zero at $x = 0.22$ but suddenly becomes finite at $x = 0.225$. This sudden appearance of a γ is in accord with the steep IM transition seen with increasing x in LCMO, while a finite γ for LSMO appears gradually by way of the intermediate state in the vicinity of the IM transition where the zero-temperature conductivity σ_0 is small but finite. Thus the appearance of the finite γ value is concomitant with the appearance of the

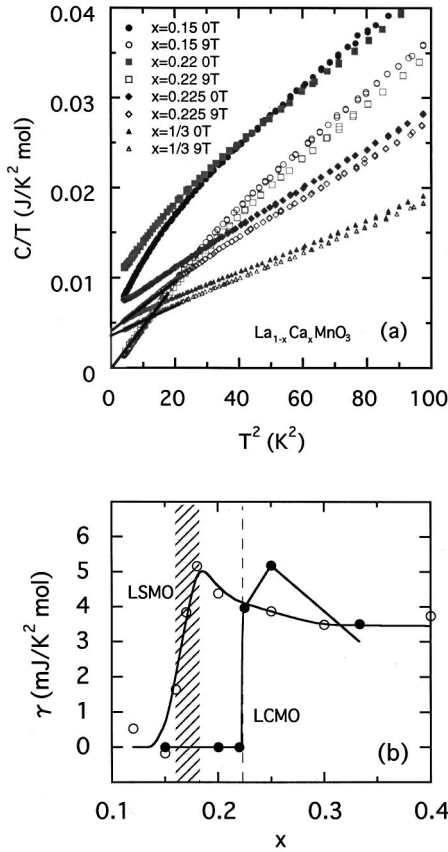


FIG. 5. (a) Temperature dependence of the specific heat measured under no magnetic field (solid symbols) and measured under 9 T (open symbols). (b) The x dependence of the electronic specific heat coefficient γ for $\text{La}_{1-x}\text{Ca}_x\text{MnO}_3$ (LCMO) and for $\text{La}_{1-x}\text{Sr}_x\text{MnO}_3$ (LSMO). For definitions of the hatched region and dashed line, see the caption of Fig. 4.

conductivity in both LCMO and LSMO. In the metallic region with x above 0.225 in LCMO the estimated γ value is 3 - 5 $\text{mJ}/\text{K}^2 \text{mol}$, which is comparable with that in the FM metallic state ($x \geq 0.18$) of LSMO.^{8,25} There is least difference, even near the IM critical region, between the γ values for LCMO and LSMO, although they have quite a different T_C value (e.g., 230 K vs 370 K around $x=0.3$). Remarkably in both the cases, the γ value does not show the clear critical enhancement near the IM transition as seen in conventional strongly-correlated-electron systems^{23,26} and changes little with x in the metallic region.

If we subtract the electronic contribution from the specific heat in an ideal FM metallic state, the residual specific heat C' consists of lattice and magnetic contributions as follows

$$C'/T^{1.5} = (C - \gamma T)/T^{1.5} = \alpha + \beta T^{1.5}. \quad (2)$$

The residual specific heat data for LCMO is plotted in Fig. 6 as $C'/T^{1.5}$ versus $T^{1.5}$. Except when $x=0.15$, the plots for data obtained at temperatures below 10 K are linear, as predicted by Eq. (2). The deviation from the linearity for $x=0.15$ is perhaps due to an occurrence of the charge/orbital ordering, which gives rise to the lower-power dependence in specific heat.²⁷ The coefficient β can be obtained from the slope of the lines in Fig. 6, and the coefficient α can be obtained by extrapolating the $C'/T^{1.5}$ value to 0 K.

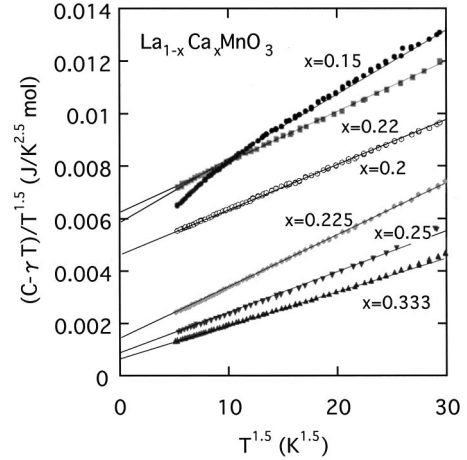


FIG. 6. Temperature dependence of the residual specific heat (the specific heat from which the electronic specific heat γT has been subtracted.) The coefficient β can be obtained from the slope of the line and the coefficient α from the extrapolated $C'/T^{1.5}$ value to 0 K (see text).

Figure 7(a) shows the coefficient β of the T^3 term, which usually represents the lattice contribution relating to the Debye temperature Θ_D (β for $x=0.15$ is estimated from the data at high temperatures). The Θ_D obtained from the coefficient β in LCMO and LSMO is plotted against x in Fig. 7(b). The Θ_D for LCMO is 340-410 K and for LSMO is 360-440 K.^{8,25} As argued in Ref. 8, the change of Θ_D with changes in x is too large to be ascribed to the change in the density. Namely, the β shows the anomalous decrease with the increase of x around the IM transition [Fig. 7(a)]. In addition, a clear increase in β is seen in the vicinity of the IM transition in LCMO. (An irregularity in the x dependence of β is also discernible around the IM transition in LSMO.)

Such an x dependence of T^3 component around the IM transition may come from the fluctuation of the orbital de-

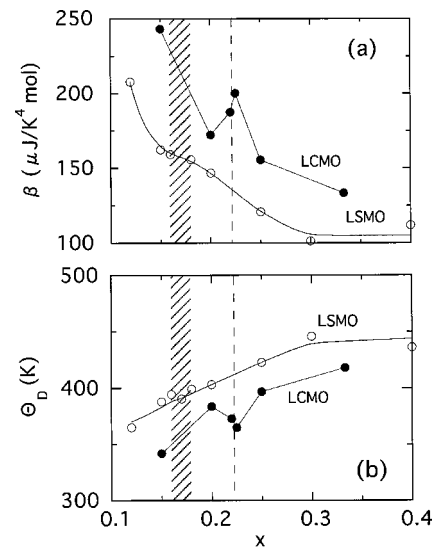


FIG. 7. For both in $\text{La}_{1-x}\text{Ca}_x\text{MnO}_3$ (LCMO) and $\text{La}_{1-x}\text{Sr}_x\text{MnO}_3$ (LSMO), the x dependence of (a) the T^3 component of the specific heat and (b) the estimated Debye temperature Θ_D . For definitions of the hatched regions and dashed line, see the caption of Fig. 4.

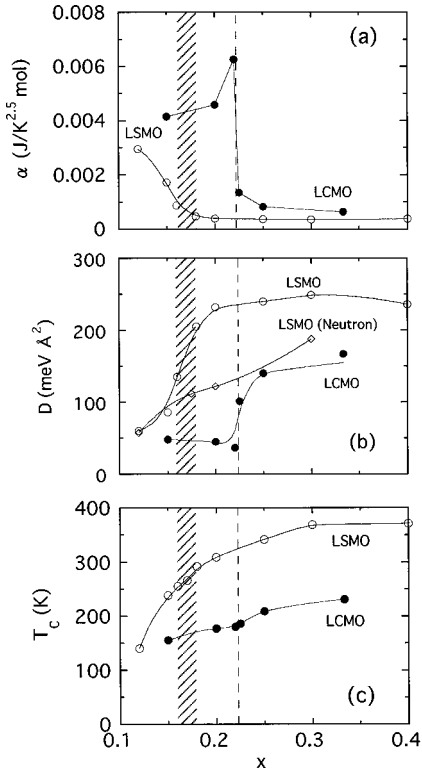


FIG. 8. The x dependence of (a) the coefficient α , (b) the estimated spin-wave stiffness constant D , and (c) the Curie temperature T_C . The values shown by diamonds (\diamond) in (b) are the values determined from the spin-wave dispersion measured in neutron scattering studies. For definitions of the hatched regions and dashed line, see the caption of Fig. 4.

gree of freedom coupled with the lattice, since there would be no other candidate, such as the 3D antiferromagnetic (AF) spin correlation, that gives rise to the T^3 component in specific heat. In a relatively wide region of x between 0.1 and 0.4 around the IM transition both in LCMO and LSMO, the critical orbital fluctuation seems to cause the phonon softening through the Jahn-Teller channel. Such a phonon softening can cause the additional lattice contribution in the specific heat, which is proportional to T^3 . Especially in the vicinity of the IM transition, the orbital fluctuation may be critically enhanced as manifested by the clear anomaly around $x = 0.22$ in LCMO, which bears analogy to the spin fluctuation at the quantum critical point between the AF metallic state and the paramagnetic metallic state.^{26,28}

In the absence of a magnetic field the spin-wave contribution in the FM state show the following $T^{1.5}$ dependence:

$$C_{spin} = \alpha T^{1.5} \approx 0.113 V k_B (k_B T / D)^{1.5}, \quad (3)$$

where V is the molar volume and D is the spin-wave stiffness constant. Figure 8 shows (a) the coefficient α estimated from the $C'/T^{1.5}$ value at 0 K in Fig. 6 and (b) the spin stiffness constant D derived from α . As seen in Fig. 8(a), the FM spin wave contribution is smaller in the insulating state than in the metallic state. Especially in LCMO α suddenly decreases at the IM transition, while in LSMO it gradually decreases through the IM transitional region. Such a low-energy spin dynamics as probed by the specific heat is thus clearly cor-

related with change in charge dynamics of the ferromagnetic ground state around the IM transition.

To clarify the spin dynamics, we show the estimated D values in Fig. 8(b). In the work reported here, we analyzed the data without assuming the spin-wave energy gap.²⁹ As seen in Fig. 6, the linearity of the plots of the residual specific heat divided by $T^{1.5}$ versus $T^{1.5}$ is good (except for LCMO with $x=0.15$), so the analysis without the spin-wave energy gap seems to be adequate. (This is also the case for LSMO.) The D values estimated from the specific heat by using Eq. (3) (D_{sp}) are shown in Fig. 8(b) in comparison with the results (D_n) of LSMO estimated by the neutron scattering measurement.²⁴ D_{sp} reflects the dispersion of the low-energy spin-wave that is thermally excited, while D_n samples the high-energy feature. In the metallic region of LSMO, D_{sp} becomes larger than D_n and is rather independent of x , while in the insulating region D_{sp} almost coincides with D_n .

The D_{sp} value for LCMO, also shown in Fig. 8(b), increases steeply at the IM transition, while the D_{sp} for LSMO seems to increase gradually in the intermediate state ($0.16 < x < 0.18$). D_{sp} is apparently related to the actual IM transition and its x -dependent change is much sharper at the IM boundary in LCMO than in LSMO. The x dependence of T_C is shown for comparison in Fig. 8(c). Although the overall behavior of D_{sp} is in accord with that of T_C as expected from the simplest model, for both LCMO and LSMO the change of D_{sp} at the IM transition is much steeper than that of T_C . These results indicate a clear difference in low-energy spin dynamics in the presence and absence of the gap in the charge sector. In other words, the origin of the ferromagnetism appears to basically differ in the insulating and metallic states: perhaps it is the superexchange interaction in the orbital-ordered insulating state and is the double-exchange interaction in the metallic state.

V. SUMMARY AND DISCUSSION

In the course of the IM transition there appear two critical features both in LCMO and LSMO. One is the critical enhancement of the magnon $T^{1.5}$ components and the lattice or orbital T^3 components in the specific heat. It manifests the critical softening of the spin-wave and the lattice mode (or orbital-wave), respectively. The latter is perhaps related to the occurrence of the orbital ordering in the insulating region adjacent to the IM phase boundary as demonstrated for LSMO.¹⁴⁻¹⁶ The other critical feature is the remnant of the orbital ordering in the FM metallic region. The resistivity upturn observed for pressurized LCMO ($x=0.22$) on the verge of the IM transition is likely attributed to the transition to the orbital-ordered state as in the case of ambient-pressure LSMO crystal.¹⁶ Even in the fully metallic region where the resistivity (ρ_0) shows roughly T^2 -temperature dependence at low temperatures, the orbital correlation is thought to persist in the form of dynamical or short-range ordering. Evidence for this is the persistence of the additional T^3 component in the specific heat after the IM transition, as is the anomalously large residual resistivity ($\rho_0 \approx 10^{-4} \Omega \text{cm}$) correlated with the T^2 coefficient of ρ . These seem to give rise to the additional scattering channel as discussed below.

As shown in Fig. 4, the T^2 coefficient A is much enhanced

near the IM transition and the A for LCMO is a few times as large as that for LSMO (Fig. 4), whereas the γ values for LCMO and LSMO are almost the same after the transitions and depend little on x (Fig. 5). Although the T^2 dependence of the resistivity and the large A coefficient seem to suggest the strong electron correlation, the ratio A/γ^2 is too large to be fit with the conventional feature of Fermi liquid such as the Kadowaki-Wood's law³⁰ and this tendency is much more pronounced in LCMO than that in LSMO. Given the near x independence of γ , the breakdown of the Kadowaki-Wood's law in this system seems to be due to the extra scattering process of carriers. The residual resistivity ρ_0 tends to gradually decrease with the decrease of the A coefficient [Fig. 4(b)]. The ρ_0 is in general proportional to the inverse of the Fermi surface area or the mean free path of the carriers. In the present case, the mean free path effect is essential, since the Hall coefficient depends little on x in the metallic region.³¹

The ground state in these manganites is 100% spin-polarized,³² so the spin fluctuation should be minimal and unable to give rise to an A value as large as the one observed in the half-metallic state. Then what gives rise to the anomalously large A coefficient? Possible contributions to the temperature dependence of resistivity are electron-magnon and electron-phonon scattering in addition to the electron-electron scattering. While for a truly half-metallic system the double magnon processes can lead to a $T^{4.5}$ temperature dependence,³³ the lower power of T (i.e., 1.5-2.5) is theoretically predicted at the low temperatures for a *nearly* half-metallic ferromagnet system³⁴ where the minority spin channel has a finite density of state at the Fermi level but does not conduct current because of the Anderson localization. We should, however, note again that the A values for both LCMO and LSMO vary largely with x , whereas the D_{sp} , Hall coefficient,³¹ and γ values for these compounds change little with the variation of x in the FM metallic region. This small variation indicates that the density of state of electrons, the area of the Fermi surface, and the excitation of magnons change little with changes in x . Thus, the simple electron-magnon scattering cannot explain the large T^2 coefficient A and its x dependence, unless one assumes a drastic change of the minority-spin density of state with the variation of x . On the other hand, the electron-phonon scattering gives a T^5 dependence of the resistivity at low temperatures, as in the case of the conventional metal, since it does not accompany spin-flip processes. Then the known framework of the electron-magnon and electron-lattice scattering cannot coherently explain all the observed experimental results.

Taking into account the critical behavior of the T^3 com-

ponent in the specific heat as mentioned above, it is natural that one should think the large A coefficient and the relevant decrease of ρ_0 are profoundly related to the excess T^3 component. In the metallic region, the both quantities are critically enhanced in the vicinity of the IM transition and gradually changes with increasing x . As discussed in Sec. IV, these behaviors strongly suggest the existence of the quantum fluctuation of the orbital. Such orbital fluctuation may qualitatively explain the excess lattice specific heat through the Jahn-Teller channel and the excess scattering channel in the transport at low temperatures, which can lead to the change of A and ρ_0 . However, it is left to be theoretically elucidated that such a specific mechanism can lead to the observed T^2 dependence of the resistivity.

VI. CONCLUSION

We have studied the features of the insulator-metal (IM) transition and the unconventional metallic ground state near the IM transition for $\text{La}_{1-x}\text{Ca}_x\text{MnO}_3$ (LCMO) single crystals and have compared them with those for $\text{La}_{1-x}\text{Sr}_x\text{MnO}_3$ (LSMO) crystals. The overall feature of transport and thermal properties seems to be qualitatively similar in LCMO and LSMO, although the anomalous features in LCMO observed with the variation of x , temperature, and hydrostatic pressure are more conspicuous than those in LSMO. The IM transition in LCMO can be caused not only by carrier doping but also by applying hydrostatic pressure. The intermediate state with the resistivity up-turn, which is realized by pressuring the LCMO ($x=0.22$) crystal, is due to the proximity of the insulating phase where for LSMO the novel orbital ordering has been confirmed to occur.¹⁴⁻¹⁸ Around the IM transition the additional magnon and T^3 components in the specific heat are enhanced perhaps by the critical fluctuation of the orbital degree of freedom coupled with the spin and lattice dynamics. The additional T^3 component of the specific heat as well as the enhancement of the T^2 coefficient A of the resistivity and the residual resistivity ρ_0 is observed in the metallic region close to the IM boundary with the minimal mass-renormalization effect, signaling the subsistence of the short-range correlation of the orbital order.

ACKNOWLEDGMENTS

We would like to thank H. Kuwahara, T. Kimura, Y. Taguchi, Y. Okimoto, and S. Miyasaka for their technical assistance and enlightening discussions. This work was supported in part by the New Energy and Industrial Technology Development Organization of Japan (NEDO).

¹For a review, see, for example, *Colossal Magnetoresistive Oxides*, edited by Y. Tokura (Gordon and Breach Science, New York, in press), and references therein.

²C. Zener, Phys. Rev. **82**, 403 (1951).

³P. W. Anderson and H. Hasegawa, Phys. Rev. **100**, 545 (1955).

⁴P.-G. de Gennes, Phys. Rev. **118**, 141 (1960).

⁵A. J. Millis, P. B. Littlewood, and B. I. Shraiman, Phys. Rev. Lett. **74**, 5144 (1995); Phys. Rev. B **54**, 5389 (1996).

⁶Y. Tokura, A. Urushibara, Y. Moritomo, T. Arima, A. Asamitsu, G. Kido, and Y. Tokura, J. Phys. Soc. Jpn. **63**, 3931 (1994); A. Urushibara, Y. Moritomo, T. Arima, A. Asamitsu, G. Kido, and Y. Tokura, Phys. Rev. B **51**, 14 103 (1995).

⁷Y. Okimoto, T. Katsufuji, T. Ishikawa, A. Urushibara, T. Arima, and Y. Tokura, Phys. Rev. Lett. **75**, 109 (1995).

⁸T. Okuda, A. Asamitsu, Y. Tomioka, T. Kimura, Y. Taguchi, and Y. Tokura, Phys. Rev. Lett. **81**, 3203 (1998).

- ⁹S. Ishihara, M. Yamanaka, and N. Nagaosa, *Phys. Rev. B* **56**, 686 (1997).
- ¹⁰M. Imada, *J. Phys. Soc. Jpn.* **67**, 45 (1998).
- ¹¹*Colossal Magnetoresistive Oxides* (Ref. 1), Chap. 7, and references therein.
- ¹²Y. Tomioka, A. Asamitsu, and Y. Tokura (unpublished).
- ¹³Y. Moritomo, A. Asamitsu, and Y. Tokura, *Phys. Rev. B* **56**, 12 190 (1997).
- ¹⁴Y. Yamada, O. Hino, S. Nohdo, R. Kanao, T. Inami, and S. Katano, *Phys. Rev. Lett.* **77**, 904 (1996).
- ¹⁵S. Uhlenbruck, R. Teipen, R. Klingeler, B. Büchner, O. Friedt, M. Hücker, H. Kierspel, T. Niemöller, L. Pinsard, A. Revcolevschi, and R. Gross, *Phys. Rev. Lett.* **82**, 185 (1999).
- ¹⁶Y. Endoh, K. Hirota, S. Ishihara, S. Okamoto, Y. Murakami, A. Nishizawa, T. Fukuda, H. Kimura, H. Nojiri, K. Kaneko, and S. Maekawa, *Phys. Rev. Lett.* **82**, 4328 (1999); H. Nojiri, K. Kaneko, M. Motokawa, K. Hirota, Y. Endoh, and K. Takahashi, *Phys. Rev. B* **60**, 4142 (1999).
- ¹⁷M. Ikebe, H. Fujishiro, and Y. Konno, *J. Phys. Soc. Jpn.* **67**, 1083 (1998).
- ¹⁸H. Fujishiro, T. Fukabe, M. Ikebe, and T. Kikuchi, *J. Phys. Soc. Jpn.* **68**, 1469 (1998).
- ¹⁹J. M. De Teresa, M. R. Ibarra, J. Blasco, J. García, C. Marquina, and P. A. Algarabel, *Phys. Rev. B* **54**, 1187 (1996).
- ²⁰V. Laukhin, J. Fontcuberta, J. L. García-Muñoz, and X. Obradors, *Phys. Rev. B* **56**, R10 009 (1997).
- ²¹To be precise, the power of T in the resistivity is slightly larger than 2 (2.1–2.2) and decreases gradually with the increase of x in the FM metallic region.
- ²²M. Jaime, P. Lin, M. B. Salamon, and P. D. Han, *Phys. Rev. B* **58**, R5901 (1998).
- ²³T. M. Rice and W. F. Brinkman, *Phys. Rev. B* **5**, 4350 (1972).
- ²⁴K. Hirota, N. Kaneko, A. Nishizawa, Y. Endoh, M. C. Martin, and G. Shirane, *Physica B* **237B-238B**, 36 (1997); Y. Endoh and K. Hirota, *J. Phys. Soc. Jpn.* **66**, 2264 (1997).
- ²⁵J. J. Hamilton, E. L. Keatley, H. L. Ju, A. K. Raychaudhuri, V. N. Smolyaninova, and R. L. Greene, *Phys. Rev. B* **54**, 14 926 (1996); B. F. Woodfield, M. L. Wilson, and J. M. Byers, *Phys. Rev. Lett.* **78**, 3201 (1997).
- ²⁶D. B. McWhan and J. P. Remeika, *Phys. Rev. B* **2**, 3734 (1970); D. B. McWhan, A. Menth, J. P. Remeika, W. F. Brinkman, and T. M. Rice, *ibid.* **7**, 1920 (1973); Y. Tokura, Y. Taguchi, Y. Okada, Y. Fujishima, T. Arima, K. Kumagai, and Y. Iye, *Phys. Rev. Lett.* **70**, 2126 (1993).
- ²⁷V. N. Smolyaninova, K. Ghosh, and R. L. Greene, *Phys. Rev. B* **58**, R14 725 (1998).
- ²⁸A. J. Millis, *Phys. Rev. B* **48**, 7183 (1993); T. Moriya, in *Spectroscopy of Mott Insulators and Correlated Metals*, edited by A. Fujimori and Y. Tokura (Springer, Berlin, 1995), pp. 66–79.
- ²⁹In a previous paper (Ref. 8) we used the D value obtained by the neutron scattering measurements (Ref. 24) to determine the spin-wave contribution to the specific heat in LSMO. In that case the field dependence of the specific heat can be explained by assuming the spin-wave energy gap Δ_{gap} for each x . The estimated Δ_{gap} value is zero in the FM insulating region below $x=0.15$ but is appreciable in the metallic region adjacent to the insulating region.
- ³⁰K. Kadowaki and S. B. Woods, *Solid State Commun.* **58**, 507 (1986).
- ³¹A. Asamitsu and Y. Tokura, *Phys. Rev. B* **58**, 47 (1998).
- ³²J.-H. Park, E. Vescovo, H.-J. Kim, C. Kwon, R. Ramesh, and T. Venkatesan, *Nature (London)* **392**, 794 (1998).
- ³³K. Kubo and N. Ohata, *J. Phys. Soc. Jpn.* **33**, 21 (1972).
- ³⁴Xindong Wang and X.-G. Zhang, *Phys. Rev. Lett.* **82**, 4276 (1999).